3 Biotech (2023) 13:414
https://doi.org/10.1007/s13205-023-03835-1

ORIGINAL ARTICLE

Reactive oxygen species induced oxidative damage to DNA, lipids, and proteins of antibiotic-resistant bacteria by plant-based silver nanoparticles

Haroon Muhammad Ali[1] · Kashmala Karam[1] · Tariq Khan[1] · Shahid Wahab[1,2] · Safi Ullah[3] · Muhammad Sadiq[3]

Received: 2 May 2023 / Accepted: 25 October 2023 / Published online: 22 November 2023

Abstract

This study assesses the mechanism of action of plant-based silver nanoparticles (AgNPs) against antibiotic-resistant bacteria. We compared AgNPs synthesized through *Salvia moorcroftiana* and *Origanum vulgare* extracts and their conjugates with the antibiotic Ceftriaxone for their capacity to cause oxidative damage through reactive oxygen species (ROS). We quantified ROS in the cells of two bacterial strains after treating them with all AgNP types and observed that AgNPs were most effective in *K. pneumoniae* as they resulted in the highest ChS1 count (44,675), while in *P. aeruginosa*, Cfx-AgNPs induced the highest levels of ROS with ChS1 count of 56,865. DNA analysis showed that both plant-based AgNPs (O-AgNPs = 0.192 and S-AgNPs = 0.152) were most effective in *K. pneumoniae* and S-AgNPs (abs = 0.174) and O-Cfx-AgNPs (abs = 0.261) in *P. aeruginosa*. We observed a significant increase in the levels of conjugated dienes (86.4 µM) and malondialdehyde (172.25 nM) in the bacterial strains after treatment with AgNPs, compared to the control (71.65 µM and 18.064 nM, respectively, in *K. pneumoniae* and *P. aeruginosa*). These results indicate lipid peroxidation. AgNPs also increased the levels of protein thiols (0.672 nM) compared to the control (0.441 nM) in *K. pneumoniae*, except for Chem-AgNPs (0.21 nM). These results suggest that plant-based AgNPs are more effective in oxidizing bacterial DNA, protein, and lipids than Chem-AgNPs. Furthermore, protein oxidation varied between AgNPs alone and AgNPs-antibiotic conjugates. The highest levels of protein thiols were found in the samples treated with O-Cfx-AgNPs (0.672 nM and 0.525 nM in *K. pneumoniae* and *P. aeruginosa,* respectively). The results demonstrated that AgNPs kill bacteria by altering bacterial macromolecules such as DNA, lipids, and proteins.

Keywords Antimicrobial potential · Cephalosporin · Macromolecules · Malondialdehyde · Nanomedicine · Phytochemicals

Introduction

Antibiotic resistance is a global concern and a constant threat to health and the economy. According to some studies, antibiotic-resistant *Pseudomonas aeruginosa* causes serious infection with a mortality rate ranging from 18% to 61% (Kang et al. 2003). Antibiotic resistance is usually caused by mutation. However, over-prescription or overuse of antibiotics pushes the bacteria to evolve and develop antibiotic resistance (Diao et al. 2022). Cephalosporin antibiotics kill bacteria by inhibiting the synthesis of peptidoglycan, a major component of the bacterial cell wall (Nie et al. 2022). Cephalosporins are known for their β-lactamase stability and their ability to easily penetrate the bacterial cell wall. Similar to other β-lactam cephalosporins, ceftriaxone exerts its mechanism of action by inhibiting cell wall synthesis through covalent binding to the penicillin-binding protein (PBP) of bacteria (Jelinkova et al. 2019). The primary factor contributing to the antibacterial effectiveness of ceftriaxone is its stability against β-lactamases. However, the excessive use of ceftriaxone has resulted in the emergence of resistance in various bacterial strains, including *Klebsiella pneumoniae* and *Pseudomonas aeruginosa*. To counteract the β-lactamase stability of ceftriaxone, bacteria have developed resistance by producing extended-spectrum β-lactamases

✉ Tariq Khan
tariqkhan@uom.edu.pk

[1] Department of Biotechnology, University of Malakand, Chakdara Dir Lower, Pakistan

[2] School of Applied Biotechnology, College of Agriculture and Convergence Technology, Jeonbuk National University, Jeonju-si, South Korea

[3] Department of Chemistry, University of Malakand, Chakdara Dir Lower, Pakistan

(Bush and Bradford 2019). Modifying the existing antibiotics or seeking new ones are merely temporary solutions. There is a requirement for multidimensional, cost-effective, and highly efficient strategies to combat multi-drug-resistant bacteria.

Nanotechnology utilizes various nanomaterials, including organic, inorganic, metallic, and non-metallic nanoparticles, to address this challenge. Nanoparticles possess unique properties such as shape, size, and surface-to-volume ratio (Gupta et al. 2019). Among inorganic metallic nanoparticles, silver (Ag), gold (Au), zinc (Zn), copper (Cu) and iron oxide (FeO) nanoparticles are widely used for their antimicrobial effects (Singh et al. 2020). Because of their better efficacy against many strains of pathogenic bacteria, AgNPs have proved to be more effective than gold, zinc, iron, copper, and other metallic nanoparticles (Shehzad et al. 2018). Chinnathambi et al. (2023) used AgNPs against Gram-negative bacterial strains; *Vibrio cholera and Escherichia coli* and found these effective against both strains of bacteria. Although, they also reported that the growth of all the strains was either slowed down or inhibited by applying different AgNPs concentrations. Akter and Huq (2020) suggested that AgNPs work like growth inhibitors against pathogenic bacteria as he studied them against *Escherichia coli* and *Staphylococcus aureus*. Tang and Zheng (2018) studied the mechanism of AgNPs against *P. aeruginosa and E. coli*. It has been discovered that these AgNPs modify the permeability of the cell wall and cell membrane, ultimately resulting in cell death. This demonstrates that AgNPs not only hinder bacterial growth but also induce their demise by compelling them to compromise the permeability of their cell wall and cell membrane. While studying the effect of the size of AgNPs on their effectiveness against bacteria, Kong et al. (2020) proved that the bactericidal effects of AgNPs increase as their sizes decrease. Biological methods, also known as green synthesis, are favored for AgNPs synthesis because they are less toxic, environment-friendly, less expensive, and require less energy (Roy et al. 2019). Given these benefits, plants, plant extracts, and phenolic compounds isolated from plants can serve as alternatives to the hazardous chemical and physical methods employed in synthesizing AgNPs. These natural sources are abundant in metabolites such as flavonoids, terpenoids, carvacrol, phenolic acids, and diverse essential oils. As a result, they have been extensively utilized for the synthesis of antibacterial AgNPs (Khafaga et al. 2020; Bano et al. 2022; Ahmed et al. 2018). Research studies suggest that AgNPs cause oxidative stress in bacteria by altering their macromolecules, such as lipids, proteins, and nucleic acid, causing lipid oxidation and protein peroxidation by producing reactive oxygen species (ROS) (Yu et al. 2020). ROS suppress the antioxidant defense causing mechanical damage to membranes through oxidation of the constituent biomolecules (Dumanović et al. 2021). This damage leads to cell membrane permeability and hence cell death. when ROS are generated, the oxygen species can weaken the hydrogen bonds and hence denaturing the double-stranded DNA (Rosli et al. 2021). Polyunsaturated fatty acids are the usual targets for lipid peroxidation because fatty acids possess multiple double bonds with reactive hydrogen atoms and are the main elements in the cell membrane components of bacteria (Xu et al. 2012). AgNPs-induced protein oxidation results in the damage of proteins either by modifying the amino side chains or resulting in the cleavage of peptide bonds, causing protein damage. Chemically synthesized AgNPs cause growth inhibition and oxidative stress in Gram-positive and Gram-negative strains of bacteria because of the higher affinity of positively charged AgNPs for the negatively charged peptidoglycan layer (Zhang et al. 2018). However, the effects of plant-based AgNPs on macromolecules such as DNA, lipids and proteins have not been assessed. In addition, less work is done on the antibacterial mechanism of plant-based AgNPs and AgNPs-antibiotic. Therefore, this study aimed to assess the effects of plant-based AgNPs induced oxidative damage to the DNA, lipids and proteins of multi-drug resistant bacteria. This study also aimed to investigate the mechanism of action of green-synthesized plant-based AgNPs against antibiotic-resistant bacteria.

Materials and methods

Biosynthesis and characterization of silver nanoparticles

Medicinal plants *S. moorcroftiana* and *O. vulgare* were collected from different areas of Swat, Khyber Pakhtunkhwa, Pakistan. A modified protocol of (Adil et al. 2019) was used for the biosynthesis of AgNPs. The identity of the plants was confirmed at the Department of Botany, University of Swat. Damaged leaves were removed, and the plants were cleaned and shade-dried for two weeks at room temperature. To prepare the extracts, the dried plants were ground into a powdered form using a regular blender. For extract preparation, 10 g of powdered plants were added to 400 mL of distilled water. The mixtures were then heated and boiled for 10 min using a magnetic stirrer hotplate. After boiling, the aqueous solution was allowed to cool down to room temperature. Subsequently, the aqueous solutions of both plants were filtered using 2.5 µm Whatman filter paper.

The filtrates were then mixed with a 4 mM solution of $AgNO_3$ in sterile flasks in 1:2 (V/V mL), respectively. The mixtures were then kept at room temperature in a place illuminated by sunlight for 3 h. The color of the reactions changed into reddish brown, which indicated the synthesis of AgNPs. The solutions were centrifuged at 13,000 rpm for 10

min in 2 mL tubes using an ultracentrifuge (model = 3K30, company = Sigma Laborzentrifugen, Germany). The supernatants were discarded, and pelleted nanoparticles were collected. The pellets were washed three times through the addition of distilled water and centrifugation. The pellets were then oven dried overnight and the AgNPs were obtained and stored for further use.

To prepare nanoparticle-antibiotic combination, 1 mL of AgNPs suspensions were mixed with 1 mL of 1mg/mL solutions of Ceftriaxone (Cfx). The solutions were then properly mixed using a vortexor followed by sonication at 20 °C for 1 h using bench-top ultrasonic cleaner (model = POWERSON I C 405, company = Hwashin technology, Korea). All the nanoparticles were characterized through UV–Vis spectroscopy, transmission electron microscopy (TEM), and energy dispersive spectroscopy (EDS) (unpublished data).

Bacterial culture

Two pathogenic Gram-negative strains of bacteria, i.e., *K. pneumoniae* (ATCC 43816) and *P. aeruginosa* (ATCC 25619), were obtained from the Institute of Basic Medical Sciences, Khyber Medical University (KMU), Peshawar. These strains were selected due to their clinical relevance and the prevalence of antimicrobial resistance observed in these species in previous literature and various antibacterial activity conducted by our colleagues (unpublished data). Both bacterial strains were cultured and sub-cultured. These subcultures were then treated with 1 mg/mL suspensions of AgNPs of both plants, their antibiotic conjugates and chemically synthesized AgNPs (Chem-AgNPs) (specific surface: 5.0 m^2/g, diameter: < 100 nm, order code 576,832-5G, Sigma–Aldrich, Steinheim, Germany) purchased from Sigma-Aldrich (Merck), adjusting the final concentration to 40 µg/mL, and the final volume was adjusted to 100 mL. These treated bacterial cultures were then incubated at 37 °C overnight in a shaking incubator at 100 rpm.

Confocal laser scanning microscopy for reactive oxygen species determination

To detect and quantify ROS levels in bacteria induced by AgNPs, the protocol of (Dwivedi et al. 2014) was followed. The Dichloro-dihydro-fluorescein diacetate (DCFDA) assay was performed. First, the bacterial cells were treated with phosphate-buffered saline (PBS). Then the cells (1 mL) were treated with 40 µg of *O. vulgare*-based AgNPs and incubated for 1 h at 37 °*C*. The samples were then washed with PBS, followed by co-inhibition in the dark with a 10 µM DCFDA for 30 min. Finally, Confocal laser scanning microscopy (CLSM) images were recorded with green fluorescence detectors. The excitation/emission (Ex/Em) wavelengths were Ex/Em = 488/521nm.

DNA damage analysis

For DNA extraction, a modified version of the protocol of (Omar et al. 2014) was followed. Broth cultures were treated with all the types of AgNPs used in this study, adjusting the final concentration to 40µg/mL (40 µg of AgNPs into 1 mL of broth). The broth cultures were then centrifuged at 13,000 rpm for 10 min. The pellets were suspended in 1 mL lysis buffer and centrifugated again at 13,000 rpm for 10 min. The pellets were resuspended in a lysis buffer and boiled for 30 min in a water bath. The samples were cooled down at room temperature and centrifuged at 13,000 rpm for 10 min. The supernatants were collected for DNA. The presence of DNA was confirmed by Gel electrophoresis. For DNA damage analysis, 500 µg/mL suspensions of DNA samples were prepared in dH_2O and were then subject to UV–Vis spectrophotometry using wavelength between 200 and 300 nm.

Lipid extraction and determination of lipid peroxidation

For lipid extraction, the protocol of (Prabakaran and Ravindran 2011) was optimized. Broth cultures were first centrifuged at 6500 rpm for 15 min. The pellets were then suspended in 1% sodium chloride (NaCl) and centrifuged at 13,000 rpm for 10 min. The pellets were then stored at −20 °C overnight. The next day, chloroform, methanol and dH_2O were added to the tubes in 1:2:0.8. Then the tubes were left still for 18 h. Lipid layers were seen the next day and collected for lipid peroxidation quantification through the following assays.

Determination of conjugated dienes

To assess the presence of conjugated dienes, the protocol of (Nadhman et al. 2016) was optimized for bacteria. The isolated lipids were first dried. 500 µg of the dried lipids were then treated with 1 mL of cyclohexane. Finally, the absorbance of all the samples was measured at 233 nm using a UV–Vis spectrophotometer. Cyclohexane alone was used as blank. The concentration of conjugated dienes was calculated using Beer-Lambert's equation which is given as $C = A/(\varepsilon \times l)$ (Where C = concentration, A = absorbance value, ε = molar absorptivity, and l = path length of the sample cell). The molar absorptivity of 2-methyl-1,3-butadiene was taken as a standard.

Malondialdehyde quantification

Malondialdehyde (MDA) was determined using a modified protocol of Thiobarbituric acid reactive substance (TBARS) assay of Tsaturyan et al. (2022). First, the lipid samples were centrifuged. The pellets were collected. For the TBARS

assay, 200 µL of Hank buffer, 200 µL of 1 mM FeSO4, and 200 µL of 1.5 mM of ascorbic acid were added to the pelleted lipids. 10% Trichloroacetic acid (TCA) and 0.357% Thiobarbituric acid (TBA) were added in 1:2 to the pellet, adjusting the final volume to 2 mL by adding dH_2O. The MDA samples were then incubated in boiling water for 15 min. The samples were centrifuged at 13,000 rpm for 10 min, and their absorbance was measured at 532 nm using a UV–Vis spectrophotometer. The TBARS solution was used as a blank. MDAs were quantified using the following formula, TBARS (µM/g) = (Ac × *V*) /*W* (where *Ac* = amount determined from the calibration curve, *W* = sample weight and *v* = total volume taken in mL.

Fourier Transform Infrared (FTIR) spectrophotometry of lipids

For investigating the effects of AgNPs on the functional groups of bacterial lipids, the FTIR protocol of (Fuller et al. 2018) was optimized. Both the treated and untreated bacterial lipids were dissolved in chloroform and analyzed using "Spectrum two FT-IR spectrometer" equipped with universal Attenuated total reflection (ATR) reflectance accessory, Potassium bromide (KBr), beam-splitter and Lithium Tantalate ($LiTaO_3$/LTO) detector. The samples were scanned at room temperature at a ratio of 1:100, and the infrared spectrum ranged between 4000 and 500 waves cm^{-1}. The spectral measurements were recorded by transmittance.

Protein extraction

The extraction method of (Fuller et al. 2018) was modified for bacterial proteins. First, the broth cultures were centrifuged at 5000 rpm for 15 min. The pellets were washed 2–3 times with PBS. 1 mL of lysozyme (1 mg/mL) in PBS was added and the mixture was sonicated for 5 min to allow cell lysis. To remove cell debris, the cells were centrifuged at 12,000 rpm for 15 min. The supernatants were collected for further extraction. Then, 1 mL TRIzol reagent was added to the supernatant, followed by the addition of 0.2 mL chloroform. The mixtures were vortexed for one minute each and then centrifuged at 12,000 rpm for 15 min at 4 °C. The upper layer with RNA was removed. Then 0.3 mL of ethanol was added for DNA precipitation and centrifuged again. The protein-containing supernatant was collected and stored for further use.

Quantification of protein thiols through Dithio-bis-(2-nitrobenzoic acid) assay

An optimized protocol by (Nadhman et al. 2016) was followed for the quantification of bacterial protein thiols. Dithio-bis-(2-nitrobenzoic acid) (DTNB) solution was prepared by adding 0.1 M phosphate buffer to 0.5 M DTNB to quantify protein thiols. 1 mL DTNB solution was then dissolved in 0.05 mL of protein solution. The absorbance of protein samples was then measured at 412 nm using a UV–Vis spectrophotometer after 30 min incubation in the dark at room temperature. DTNB dissolved in deionized water was used as a blank. Proteins dissolved in phosphate buffer were used as control. Protein thiols were quantified using the formula; absorbance change = DTNB treated proteins – control—blank. These values were then multiplied by a factor of 21 to give thiol concentration in moles per litre.

Statistical analysis

The experiments were conducted using a completely randomized design. Each experiment was repeated twice to ensure reliability, and each treatment was performed three times (triplicates). Statistical analyses were carried out using SPSS 20 and Microsoft Excel 2019. For determining significant mean differences, linear regression analysis was employed. A significance level of $p < 0.05$ was used to identify statistically significant results. All figures were generated using Origin 8.5 software.

Results

Reactive oxygen species quantification

ROS quantification was performed to understand the oxidative effect of AgNPs on bacteria. For this purpose, *K. pneumoniae* and *P. aeruginosa* were treated with AgNPs and Cfx-AgNPs, and the fluorescence intensity of both samples was measured using CLSM. The fluorescence intensity shows that both AgNPs and Cfx-AgNPs induced high levels of ROS in both strains, as shown in Figs. 1 and 2. Figure 1 shows the highest fluorescence intensity in AgNPs and intermediate in Cfx-AgNPs meaning that AgNPs induced higher levels of ROS than Cfx-AgNPs in *K. pneumoniae, while* Cfx-AgNPs were found to induce the highest levels of ROS in *P. aeruginosa.* Similarly, according to histograms a and b, AgNPs were most effective in *K. pneumoniae* as they resulted in the highest ChS1 count (44,675), while in *P. aeruginosa*, Cfx-AgNPs induced the highest levels of ROS with ChS1 count of 56,865 (Fig. 3).

DNA damage analysis

Results showed the potentials of chemically-synthesized AgNPs (Chem-AgNPs), plant-based AgNPs, i.e., *S. moorcoftiana* (S-AgNPs) and *O. vulagare* (O-AgNPs) alone and in conjugation with Ceftriaxone such as S-Cfx-AgNPs (*S. moorcroftiana*-cefriaxone AgNPs*)* and O-Cfx-AgNPs *(O.*

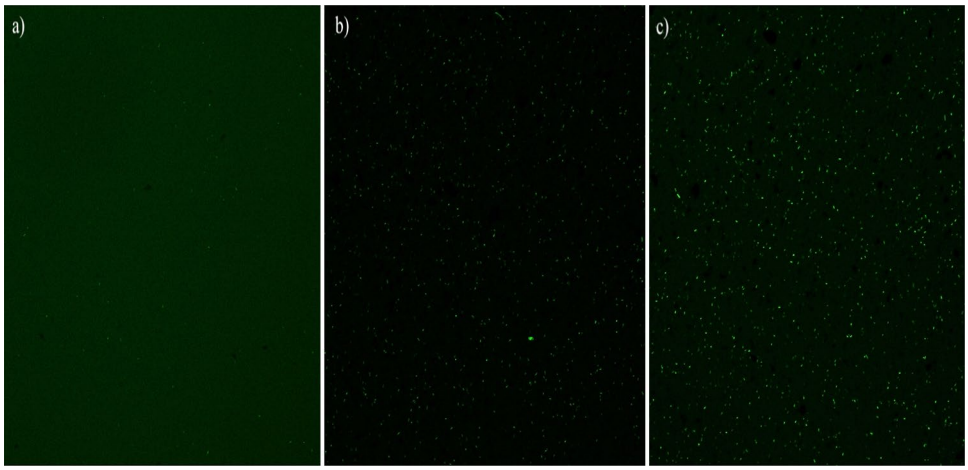

Fig. 1 Fluorescence microscopy images showing increased fluorescence intensity in *Klebsiella pneumoniae* treated with AgNPs (**b**) and Cfx-AgNPs (**c**) compared to control (**a**)

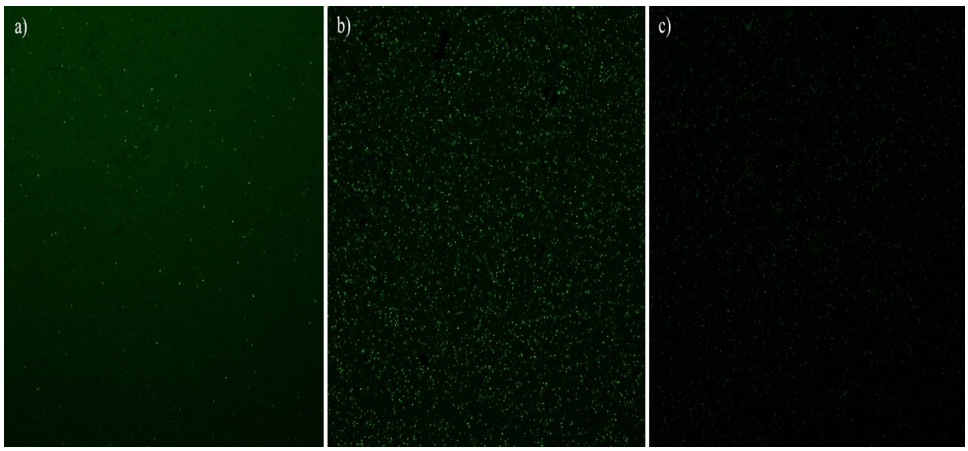

Fig. 2 Fluorescence microscopy images showing increased fluorescence intensity in *Pseudomonas aeruginosa* when treated with AgNPs (**b**) and Cfx-AgNPs (**c**) compared to control (**a**)

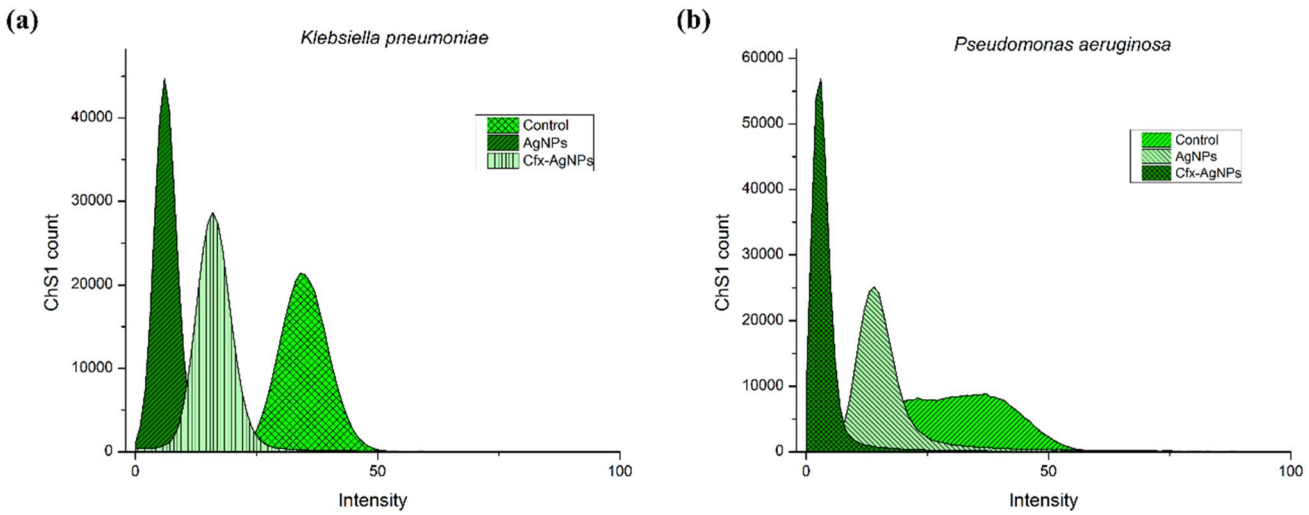

Fig. 3 Increased levels of ChS1 indicating increased ROS levels in *Klebsiella pneumoniae* and *Pseudomonas aeruginosa* treated with AgNPs and Cfx-AgNPs

Vulgare-ceftriaxone AgNPs*)* to damage the DNA of *K. pneumoniae* and *P. aeruginosa*. The results show that all types of AgNPs significantly reduced DNA in both bacterial strains when compared to control (untreated DNA suspensions) (0.211 and 0.612 at 280 nm in *K. pneumoniae* and *P. aeruginosa* respectively), except O-Cfx-AgNPs (abs = 0.261 at 280 nm) and Chem-AgNPs (abs = 0.241), which were not effective in inducing DNA damage in *K. pneumoniae*. In *K. pneumoniae,* both plant-based AgNPs (O-AgNPs = 0.192 and S-AgNPs = 0.152) were more effective than Chem-AgNPs (abs = 0.121) and Cfx-AgNPs (abs = 0.086), as shown in Fig. 4. While in *P. aeruginosa,* S-AgNPs (abs = 0.174) and O-Cfx-AgNPs (abs = 0.261) were most effective, as shown in Fig. 5. Chem-AgNPs showed the least activity in *K. pneumoniae* and intermediate in *P. aeruginosa.*

Analysis of lipid oxidation

Quantification of conjugated dienes

Conjugated dienes are double-bonded lipid molecules separated by single bonds. They are formed when the ROS

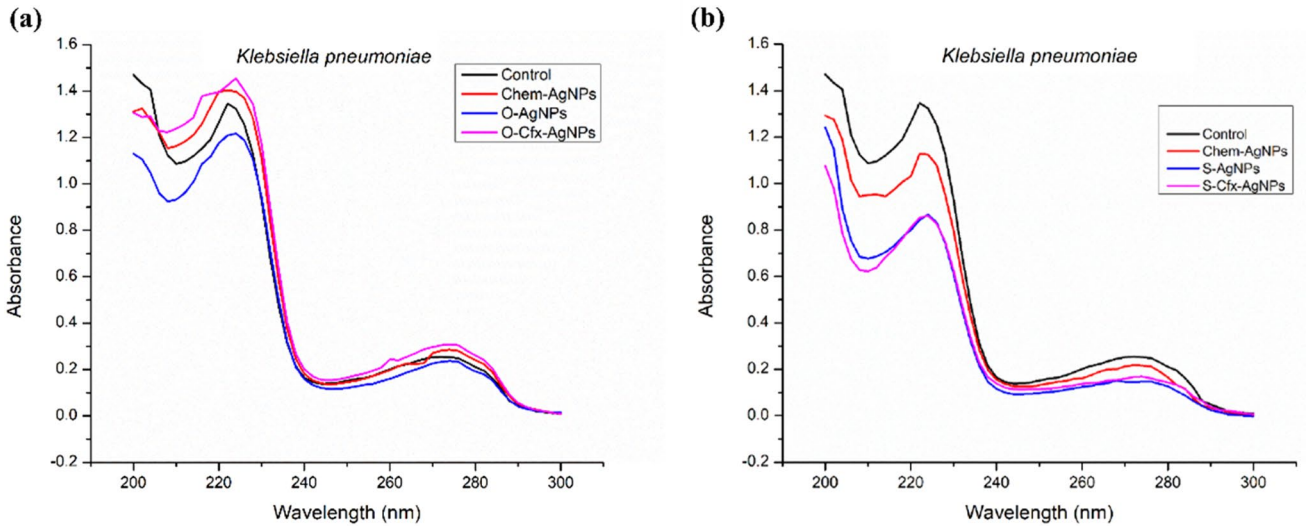

Fig. 4 The levels of DNA decreased more significantly after treating *Klebsiella pneumoniae* with O-AgNPs, O-Cfx-AgNPs (**a**), S-AgNPs, and S-Cfx-AgNPs (**b**) than Chem-AgNPs

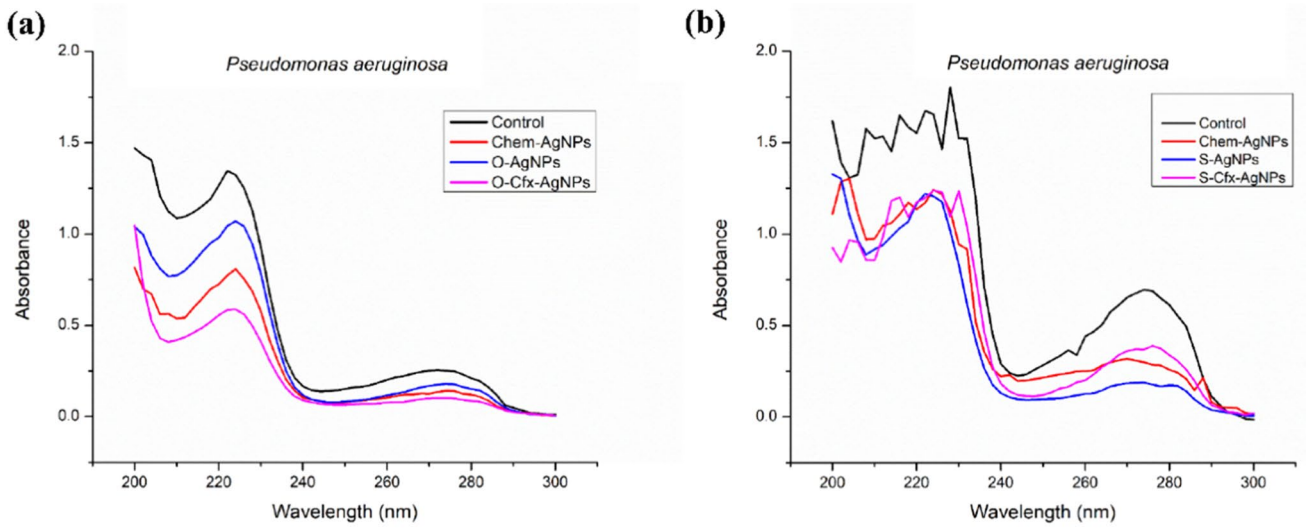

Fig. 5 The levels of DNA decreased more significantly after treating *Pseudomonas aeruginosa* with O-AgNPs, O-Cfx-AgNPs (**a**), S-AgNPs, and S-Cfx-AgNPs (**b**) than Chem-AgNPs

induced by AgNPs oxidize the lipids of bacteria. This study determined the extent of conjugated dienes after treating them with Chem-AgNPs, O-AgNPs, S-AgNPs, and Cfx-AgNPs. In *K. pneumoniae,* the highest level of conjugated dienes was resulted by O-AgNPs (76.7 µM), followed by S-Cfx-AgNPs (75.45 µM) and O-Cfx-AgNPs (75.05 µM) when compared to control (43.9 µM), while Chem-AgNPs (15.2 µM) was the least effective as shown in Fig. 6a. Figure 6b showed that the highest levels of conjugated dienes were resulted by S-Cfx-AgNPs (86.4 µM) followed by O-Cfx-AgNPs (74.45 µM) and O-AgNPs (74.35 µM) in *Pseudomonas aeruginosa*. The lowest levels of conjugated dienes were induced by S-AgNPs (51.7 µM), while control is 66.35 µM. The figures suggest that the AgNPs alone are the most effective in *K. pneumoniae* and least effective in *P.aeruginosa*.

Quantification of malondialdehydes

MDA is the final byproduct of the lipid peroxidation reaction. It is an indicator of lipid peroxidation extent. The levels of MDA were determined after treating them with Chem-AgNPs, O-AgNPs, O-Cfx-AgNPs, S-AgNPs and S-Cfx-AgNPs. The results of MDA quantification showed that all AgNPs increased MDA content in *K. pneumoniae* and *P. aeruginosa* compared to untreated bacterial cells (controls) (18.06452 nM and 16.77419 nM, respectively). Figure 7a showed that S-AgNPs (172.25806 nM) induced the highest levels of MDA content in *K. pneumoniae,* followed by O-AgNPs and S-Cfx-AgNPs with 131.6129 nM of MDA each. While the lowest levels of MDA were resulted by Chem-AgNPs (19.35484 nM). In *P. aeruginosa,* O-AgNPs with 50.32258 nM were most effective as shown in Fig. 7b. S-AgNPs (42.58064 nM) also induced MDA more significantly than O-Cfx-AgNPs (21.29032 nM) and S-Cfx-AgNPs (20 nM). However, all the AgNPs samples were more effective than Chem-AgNPs (19.354839 and 17.419355 in *K. pneumoniae* and *P. aeruginosa,* respectively).

Fourier Transform Infrared spectrometry (FTIR) of bacterial lipids

FTIR of all the samples was done to investigate the effects of AgNPs and their conjugates with cephalosporins on the functional groups of bacterial lipids. For this purpose, the lipid samples were treated with O-AgNPs, O-Cfx-AgNPs, S-AgNPs, S-Cfx-AgNPs and Chem-AgNPs and were compared to control (untreated lipid) samples for functional group analysis. The results show that the transmittance of all the treated lipid samples increased to 65.4% between 742–709 cm-1 when compared to the untreated bacterial lipids with 54.7% transmittance of light. It means that only the C-H bonds in the hydrocarbon chain of bacterial lipids are compromised, as shown in Fig. 8.

Quantification of protein oxidation

Thiols are produced because of amino acid oxidation caused by AgNPs-induced ROS. The levels of thiols formed when treated with AgNPs indicate the effects of these AgNPs on bacterial proteins. We treated the isolated bacterial proteins with Chem-AgNPs, O-AgNPs, and S-AgNPs and their conjugates with ceftriaxone (O-Cfx-AgNPs and S-Cfx-AgNPs) and compared the levels of protein thiols induced by these

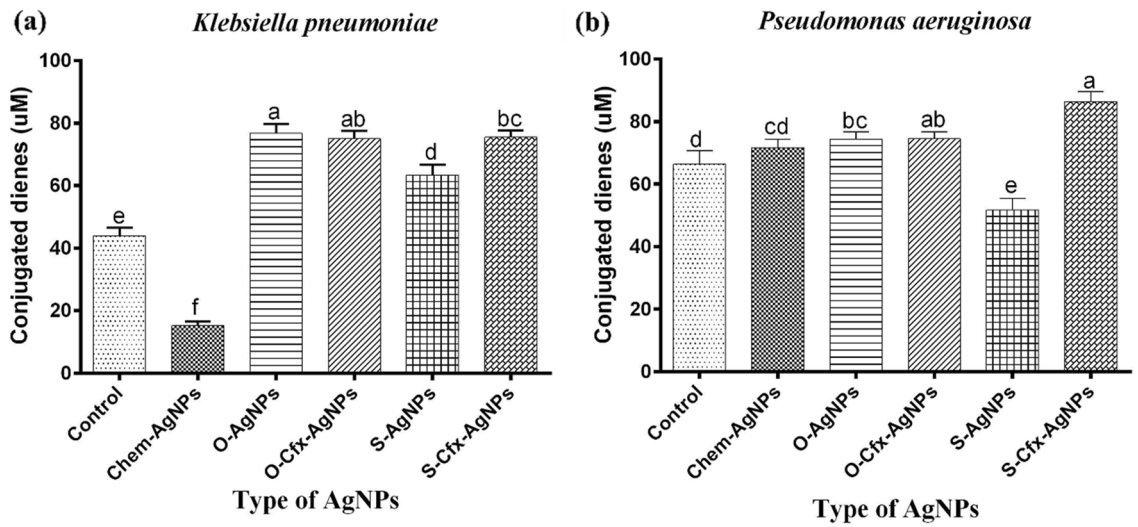

Fig. 6 The levels of conjugated dienes increased significantly in *Klebsiella pneumoniae* (**a**) and *Pseudomonas aeruginosa* (**b**) when treated with Chem-AgNPs, O-AgNPs, O-Cfx-AgNPs, S-AgNPs and S-Cfx-AgNPs

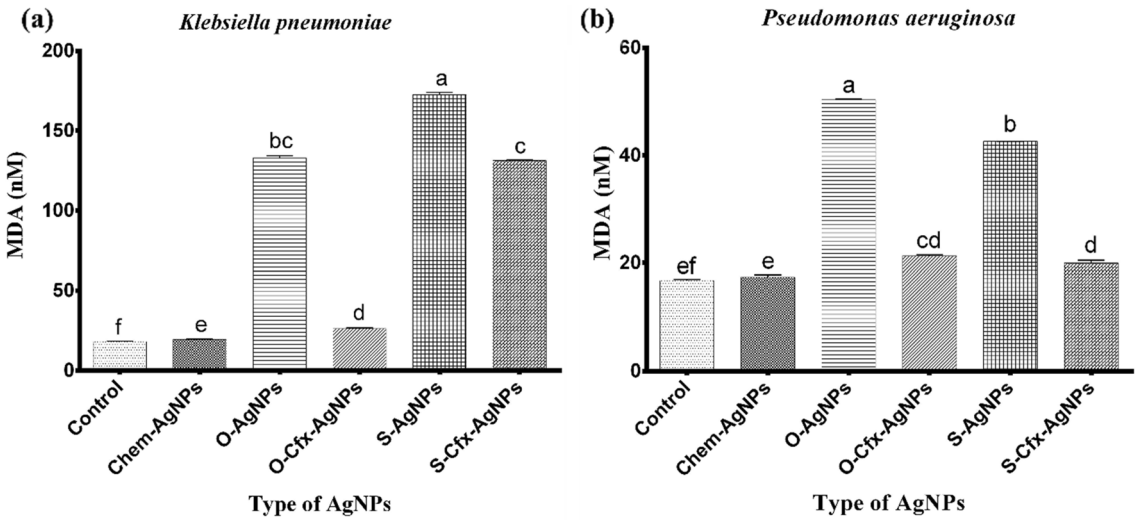

Fig. 7 The levels of MDA content increased significantly in *Klebsiella pneumoniae* (**a**) and *Pseudomonas aeruginosa* (**b**) after treating with Chem-AgNPs, O-AgNPs, O-Cfx-AgNPs, S-AgNPs and S-Cfx-AgNPs

samples with untreated bacterial proteins (controls) (0.441 nM and 0.378 nM in *K. pneumoniae and P. aeruginosa*). In *K. pneumoniae*, O-AgNPs (0.588 nM) and its conjugate O-Cfx-AgNPs (0.672 nM) induced more protein thiols than S-AgNPs (0.462 nM) and its conjugate S-Cfx-AgNPs (0.525 nM) as shown in Fig. 9a. Similarly, Fig. 9b showed that in *P. aeruginosa,* O-AgNPs (0.462 nM) and its conjugate O-Cfx-AgNPs (0.525 nM) were more effective than S-AgNPs (0.377 nM) and its conjugate S-Cfx-AgNPs (0.392 nM). However, Chem-AgNPs were found to be least effective in both the strains with 0.21 nM of protein thiols induced.

Discussion

The antimicrobial applications of plant-based AgNPs have captivated researchers. Due to their unique characteristics, such as shape, size, and surface-to-volume ratio, AgNPs have been a focal point of research in recent decades, aiming to find environment-friendly, cost-effective, and less toxic alternatives to antibiotics in combating antibiotic resistance. The antibacterial activity of AgNPs has been extensively documented in previous studies. In our study, we investigated the antibacterial mechanisms of AgNPs synthesized from the aqueous extracts of *Origanum vulgare* (O-AgNPs) and *Salvia moorcroftiana* (S-AgNPs), as well as their conjugates with Ceftriaxone (O-Cfx-AgNPs and S-Cfx-AgNPs).

The most extensively studied mechanism of AgNPs is likely the oxidative damage to bacterial lipid and protein membranes, induced by AgNPs-generated ROS (Ramzan et al. 2022), which serves as the primary hypothesis of our study. Both AgNPs and Cfx-AgNPs induced elevated levels of ROS in *K. pneumoniae* and *P. aeruginosa*, subsequently resulting in oxidative damage to the protein and lipid membranes of these bacterial strains, ultimately leading to bacterial cell death (Ameh et al. 2022). However, the levels of effectiveness varied among AgNPs and Cfx-AgNPs, indicating the importance of considering the resistance profiles of bacterial strains, the role of phytochemicals in the antibacterial activity of plant-based AgNPs, and the synergistic effects of AgNPs and antibiotics in designing therapeutic interventions. The results demonstrate that AgNPs were the most effective against *K. pneumoniae*, whereas Cfx-AgNPs exhibited higher efficacy against *P. aeruginosa*. This discrepancy may be attributed to the inherent resistance of *K. pneumoniae* to cephalosporins and the reduced oxidative potential of AgNPs when conjugated with cephalosporin antibiotics. This observation is also supported by the disc diffusion antibacterial activities in our lab (unpublished data). On the other hand, while *P. aeruginosa* is not as resistant to cephalosporins as *K. pneumoniae*, the oxidative effect of AgNPs is enhanced upon conjugation with cephalosporin antibiotics. This suggests a potential synergistic effect between the oxidative properties of AgNPs and the antibacterial activity of β-lactamases against Gram-negative strains.

We investigated the effects of oxidative stress as a potential antibacterial mechanism of AgNPs and their conjugates on bacterial DNA. The reduced levels of DNA in both bacterial strains indicated the DNA-damaging effects of the AgNPs used in our study. This conclusion was drawn based on the observed decrease in DNA levels in both strains when treated with all the AgNPs suspensions from our study, compared to the untreated bacterial suspensions (control). These findings are consistent with a previous study (Abbas et al. 2019), which reported significant DNA-damaging activity in Gram-negative bacterial strains. It is noteworthy that

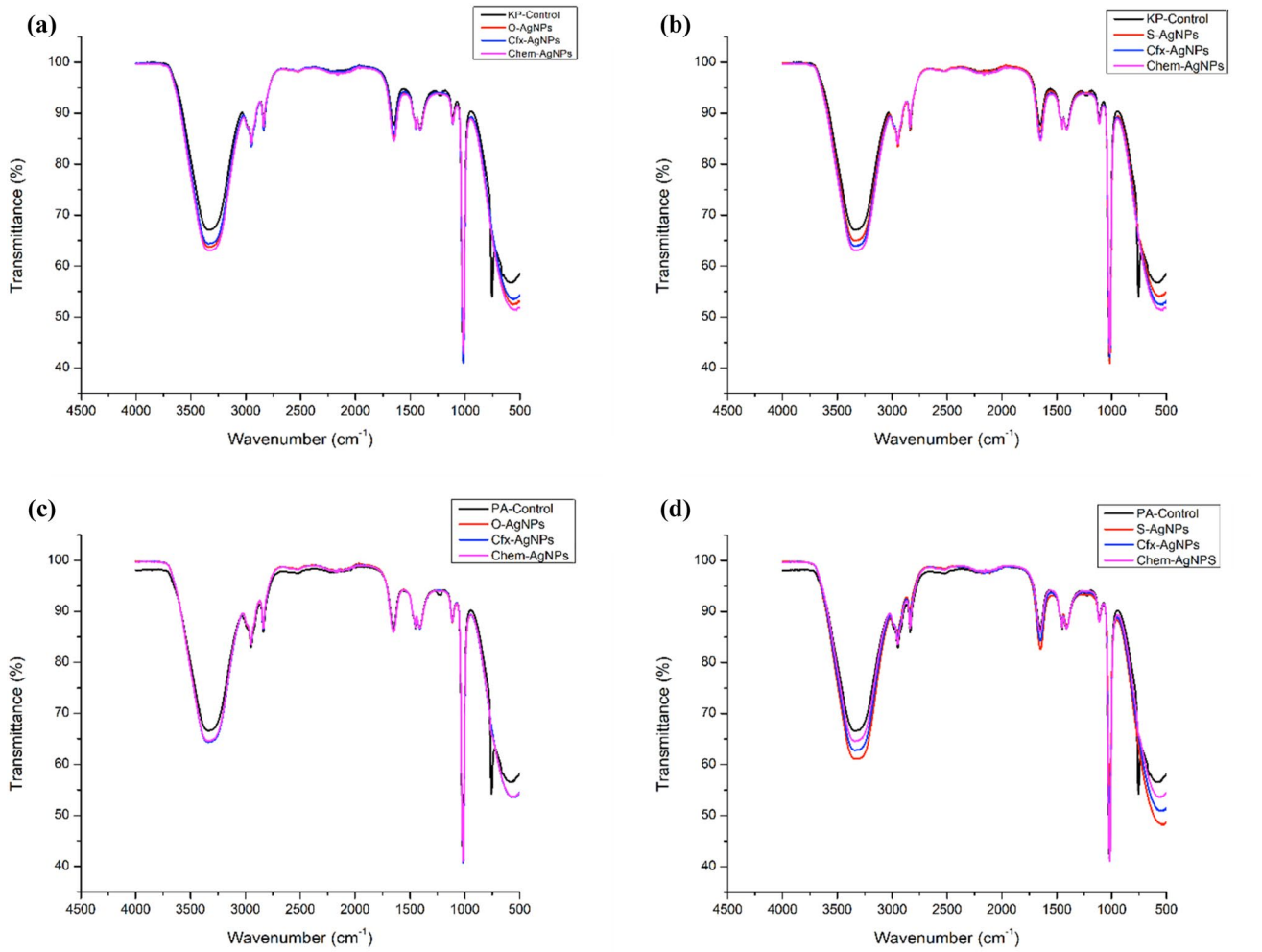

Fig. 8 FTIR spectra of O-AgNPs, O-Cfx-AgNPs, S-AgNPs, S-Cfx-AgNPs and Chem-AgNPs used to study the changes in the transmittance of *Klebsiella pneumoniae* (**a** and **b**) and *Pseudomonas aeruginosa* (**c** and **d**) lipids in the spectral range of 742–709 cm^{-1} suggesting changes in their functional groups

the efficacy of all plant-based AgNPs was highest, except for O-AgNPs in *K. pneumoniae*. We hypothesize that the increased sizes of AgNPs upon conjugation might contribute to this observation, as nanoparticle size plays a crucial role in their antibacterial activity. These findings are consistent with the results previously reported by Muenraya et al. (2022) which indicated that the DNA degradation activity of AgNPs decreases with increasing size. However, all green-synthesized AgNPs and their conjugates exhibited more significant DNA-damaging activity than chemically synthesized AgNPs. This difference may be attributed to the presence of various phytochemicals and flavonoids with antibacterial and antioxidant potential in *O. vulgare* and *S. moorcroftiana* (Irfan and Qadir 2017; Saeed and Tariq 2009).

We evaluated lipid peroxidation as an indicator of oxidative stress induced by AgNPs. AgNPs cause bacterial cell death either by apoptosis or necrosis (Devanesan et al. 2021). Lipid peroxidation is one of the most convincing oxidative stress pathways as an antibacterial mechanism of AgNPs. Consistent with the previous study of (Adeyemi et al. 2020), our results showed significant lipid peroxidation of bacteria by AgNPs. Specifically, the results show that S-Cfx-AgNPs exhibited higher activity than S-AgNPs in *P. aeruginosa*. This is because of the combined activity of carvacrol-rich *S. moorcroftiana* and antibiotics. Carvacrol has been previously reported as a major constituent of *S. moorcroftiana* by Zhao et al. (2019) to cause significant lipid peroxidation in bacteria indicating that carvacrol has the potential to alter the lipid bilayer hence compromising the cell membrane integrity of bacteria. Similarly, S-AgNPs were less effective than S-Cfx-AgNPs in *K. pneumoniae*, while O-AgNPs and O-Cfx-AgNPs were almost equally effective in both strains. This underscores the importance

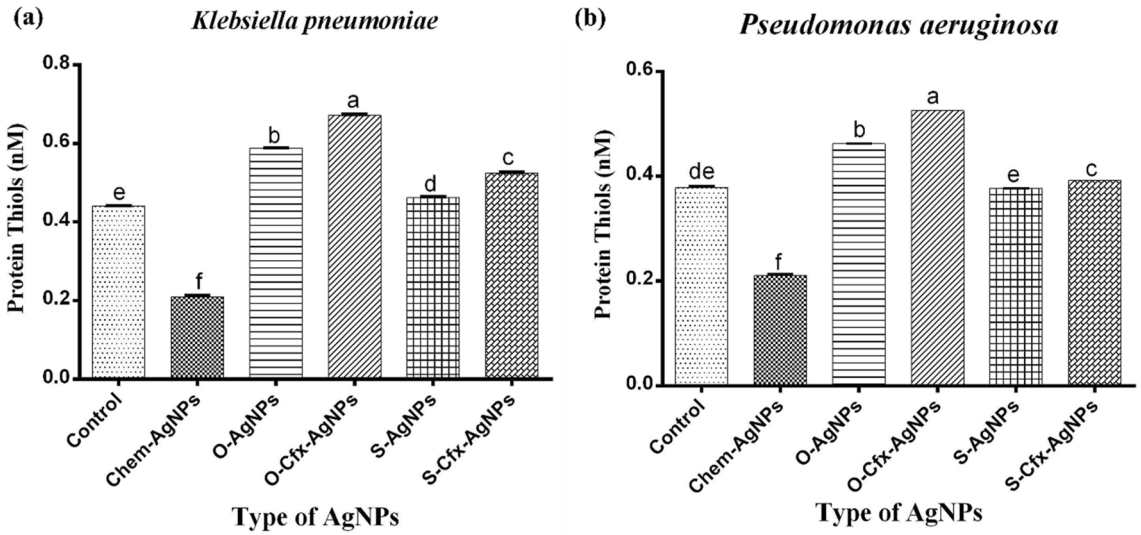

Fig. 9 Increased levels of protein thiols were observed in *Klebsiella pneumoniae* (**a**) and *Pseudomonas aeruginosa* (**b**) when treated with Chem-AgNPs, O-AgNPs and O-Cfx-AgNPs, S-AgNPs and S-Cfx-AgNPs

of the synthesis methods of AgNPs. However, most of the nanoparticles displayed greater lipid peroxidation activity than chemically synthesized AgNPs, from which we concluded the enhanced efficacy of green-synthesized AgNPs and their conjugates, suggesting that they hold the promise to be more effective triggering agents of lipid peroxidation compared to chemically synthesized AgNPs. This distinction is due to the presence of specific bioactive compounds in plants such as *S. moorcroftiana* combined with the bactericidal effects of cephalosporins.

MDA quantification was done to assess the extent of lipid peroxidation as MDA is the end byproduct of the lipid peroxidation reaction (Effendi et al. 2022). It is known as a lipid peroxidation marker because MDA content indicates the completion of the lipid peroxidation reaction (Trombetti et al. 2022). In accordance with the previously reported study of Quinteros et al. (2018), we observed that MDA content increased when treated with AgNPs compared to the untreated bacterial cells (control) in Gram-negative bacteria. We concluded from these results that AgNPs significantly induce MDA accumulation in bacterial cells, indicating the successful lipid peroxidation of Gram-negative bacteria. However, the magnitude of significance varied between different AgNPs types. Specifically, O-AgNPs and S-AgNPs increased the MDA content more significantly than their respective antibiotic conjugates: O-Cfx-AgNPs and S-Cfx-AgNPs. This could either be attributed to the increased bacterial lipid peroxidation potency of AgNPs a little, or to the increased size of AgNPs-antibiotic conjugate limiting the cell membrane disruption and penetration of AgNPs. However, both AgNPs alone and their conjugates increased MDA content more than Chem-AgNPs. It can be concluded that green-synthesized AgNPs have superior antibacterial potential than chemically synthesized AgNPs. These findings also highlight the importance of AgNPs synthesis methods in modulating their effectiveness.

FTIR analysis showed a significant difference in the transmittance of treated and untreated bacterial lipids in the spectral range of 742–709 cm^{-1}. Between, 742–709 cm^{-1}, the transmittance of the untreated bacterial lipids was 54.4%, which increased to 65.4% when treated with AgNPs and its conjugates shedding light on the significant alterations in the molecular compositions of bacterial lipids. This variation in the intensity signifies the modifications in the vibrational modes of chemical bonds in lipids, as the difference in the absorption and transmission of infrared light by C-H and hydroxyl (OH) functional groups is measured by FTIR spectroscopy. This shift in the transmittance indicates that OH groups replaced the C-H groups which signifies the initiation of lipids peroxidation. The presence of OH groups is due to the formation of oxidized groups breaking the carbon–carbon double bonds in the hydrocarbon chain. Also, the significant increase in the transmittance when treated with AgNPs and conjugates is evidence of high concentrations of lipid peroxidation products. The same results were also reported in the study of (Gutteridge and Halliwell 1990), who concluded that the substitution of C-H groups by OH serves as the initial stage of lipid peroxidation within the hydrocarbon chain of unsaturated fatty acids when treated with nanoparticles, disrupting the integrity and functionality of bacterial lipid membranes. This disruption may lead to bacterial cell death due to structural instability and compromised permeability. These results reveal evidence of lipid peroxidation,

corroborating the results obtained from conjugated dienes quantification and MDA in our study.

We also assessed protein peroxidation as a measure of the oxidative effects of AgNPs on the proteins of Gram-negative bacteria. Protein oxidation is another oxidative stress pathway of AgNPs. Protein oxidation is an oxidation reaction involving the oxidation of protein molecules by ROS, leading to the degradation of proteins (Zhou et al. 2022). Oxidative stress is caused by the alteration of protein composition by AgNPs-induced ROS, resulting in bacterial cell death (Gruber et al. 2022). Protein thiols are organic compounds like alcohols and phenols, however, they contain sulfur molecules in their side chains instead of oxygen. Only cysteine amino acids have side chains with thiol groups. Protein thiols are also the byproducts of protein oxidation reaction and are, therefore, very unstable and further oxidize protein molecules, thereby contributing to the oxidative stress (Demirci-Çekiç et al. 2022). After treating bacterial proteins with all AgNPs samples, we determined the levels of leaked thiols to determine the extent of protein oxidation. Because the increased level of thiols reflects the activation of oxidative stress pathways and subsequent oxidation of proteins. According to the results, all AgNPs increased levels of thiols than those of untreated bacterial cells (control) except Chem-AgNPs. These results demonstrate that plant-based AgNPs are more active in oxidizing bacterial protein than Chem-AgNPs. However, the significance varied between AgNPs alone and AgNPs-antibiotic conjugates. The results showed that AgNPs-antibiotic conjugates increased thiol levels more significantly than AgNPs alone, which indicates that the conjugation of AgNPs with antibiotics increased the oxidative effects of AgNPs on bacterial proteins. This was probably because of the combined bactericidal effects of AgNPs and antibiotics in the conjugates.

Conclusion

O. vulgare and S. moorcroftiana's extracts based silver nanoparticles showed significant antibacterial activity alone and in synergism with their Ceftriaxone conjugates against Gram-negative bacterial strains. The study concludes that the main antibacterial mechanism of AgNPs is causing oxidative damage to bacterial membranes by inducing reactive oxygen species (ROS). The induction of ROS by AgNPs and their conjugates leads to DNA, lipid and protein damage in bacteria, ultimately resulting in cell death. The study also revealed that green-synthesized AgNPs have superior antibacterial potential compared to chemically-synthesized AgNPs. These findings highlight that plant-based AgNPs and their conjugates with antibiotics hold the promise to be utilized as potential nanomedicine and address the global concern of antibiotic resistance by combating multidrug-resistant bacteria. However, further research is required to fully investigate and unravel the antimicrobial mechanisms of AgNPs, their toxicity minimization and their application in clinical settings.

Funding International foundation for science, IFS F 6455-1, Tariq Khan.

Declarations

Conflict of interest All the authors declare no conflict of interests.

Ethical approval Not applicable.

References

Abbas WS, Atwan ZW, Abdulhussein ZR, Mahdi M (2019) Preparation of silver nanoparticles as antibacterial agents through DNA damage. Mater Technol 34(14):867–879

Adeyemi OS, Shittu EO, Akpor OB, Rotimi D, Batiha GE-s, (2020) Silver nanoparticles restrict microbial growth by promoting oxidative stress and DNA damage. EXCLI J 19:492

Adil M, Khan T, Aasim M, Khan AA, Ashraf M (2019) Evaluation of the antibacterial potential of silver nanoparticles synthesized through the interaction of antibiotic and aqueous callus extract of Fagonia indica. AMB Express 9(1):1–12

Ahmed B, Hashmi A, Khan MS, Musarrat J (2018) ROS mediated destruction of cell membrane, growth and biofilms of human bacterial pathogens by stable metallic AgNPs functionalized from bell pepper extract and quercetin. Adv Powder Technol 29(7):1601–1616

Akter S, Huq MA (2020) Biologically rapid synthesis of silver nanoparticles by Sphingobium sp. MAH-11T and their antibacterial activity and mechanisms investigation against drug-resistant pathogenic microbes. Artif Cells Nanomed Biotechnol 48(1):672–682

Ameh T, Gibb M, Stevens D, Pradhan SH, Braswell E, Sayes CM (2022) Silver and copper nanoparticles induce oxidative stress in bacteria and mammalian cells. Nanomaterials 12(14):2402

Bano AS, Khattak AM, Basit A, Alam M, Shah ST, Ahmad N, Gilani SAQ, Ullah I, Anwar S, Mohamed HI (2022) Callus induction, proliferation, enhanced secondary metabolites production and antioxidants activity of *Salvia moorcroftiana* L. as Influenced by Combinations of Auxin, cytokinin and melatonin. Braz Arch Biol Technol 65:e22210200

Bush K, Bradford PA (2019) Interplay between β-lactamases and new β-lactamase inhibitors. Nat Rev Microbiol 17(5):295–306

Chinnathambi A, Alharbi SA, Joshi D, Saranya V, Jhanani G, On-Uma R, Jutamas K, Anupong W (2023) Synthesis of AgNPs from leaf extract of Naringi crenulata and evaluation of its antibacterial activity against multidrug resistant bacteria. Environ Res 216:114455

Demirci-Çekiç S, Özkan G, Avan AN, Uzunboy S, Çapanoğlu E, Apak R (2022) Biomarkers of oxidative stress and antioxidant defense. J Pharm Biomed Anal 209:114477

Devanesan S, Jayamala M, AlSalhi MS, Umamaheshwari S, Ranjitsingh AJA (2021) Antimicrobial and anticancer properties of Carica papaya leaves derived di-methyl flubendazole mediated silver nanoparticles. J Infect Public Health 14(5):577–587

Diao J, Li M, Zhang P, Zong C, Ma W, Ma L (2022) Overexpression of the PdpapERF109 gene enhances resistance of Populus davidiana P. alba var pyramidalis to Fusarium oxysporum infection. J for Res 33(6):1925–1937

Dumanović J, Nepovimova E, Natić M, Kuča K, Jaćević V (2021) The significance of reactive oxygen species and antioxidant defense system in plants: A concise overview. Front Plant Sci 11:552969

Dwivedi S, Wahab R, Khan F, Mishra YK, Musarrat J, Al-Khedhairy AA (2014) Reactive oxygen species mediated bacterial biofilm inhibition via zinc oxide nanoparticles and their statistical determination. PLoS ONE 9(11):e111289

Effendi AN, Iswahyudi M, Cho E, Kumala S, Sinaga E (2022) Supplementation of Bouea macrophylla fruit juice prevent oxidative stress in rats fed with high-fat high-cholesterol diet through attenuation of lipid peroxidation. Int J Biol Phys Chem Stud 4(2):20–29

Fuller ME, Andaya C, McClay K (2018) Evaluation of ATR-FTIR for analysis of bacterial cellulose impurities. J Microbiol Methods 144:145–151

Gruber CC, Babu VM, Livingston K, Joisher H, Walker GC (2022) Degradation of the *Escherichia coli* essential proteins DapB and Dxr results in oxidative stress, which contributes to lethality through incomplete base excision repair. Mbio 13(1):e03756-e13721

Gupta A, Mumtaz S, Li C-H, Hussain I, Rotello VM (2019) Combatting antibiotic-resistant bacteria using nanomaterials. Chem Soc Rev 48(2):415–427

Gutteridge JM, Halliwell B (1990) The measurement and mechanism of lipid peroxidation in biological systems. Trends Biochem Sci 15(4):129–135

Irfan M, Qadir MIJPJPS (2017) Analgesic, anti-inflammatory and antipyretic activity of Salvia moorcroftiana. Pak J Pharm Sci 30(2):481–486

Jelinkova P, Mazumdar A, Sur VP, Kociova S, Dolezelikova K, Jimenez AMJ, Koudelkova Z, Mishra PK, Smerkova K, Heger Z (2019) Nanoparticle-drug conjugates treating bacterial infections. J Control Release 307:166–185

Kang C-I, Kim S-H, Kim H-B, Park S-W, Choe Y-J, Oh M-d, Kim E-C, Choe K-WJCid, (2003) Pseudomonas aeruginosa bacteremia: risk factors for mortality and influence of delayed receipt of effective antimicrobial therapy on clinical outcome. Clin Infect Dis 6:745–751

Khafaga AF, Naiel MA, Dawood MA, Abdel-Latif HM (2020) Dietary Origanum vulgare essential oil attenuates cypermethrin-induced biochemical changes, oxidative stress, histopathological alterations, apoptosis, and reduces DNA damage in common carp (Cyprinus carpio). Aquat Toxicol 228:105624

Kong IC, Ko K-S, Koh D-C (2020) Evaluation of the effects of particle sizes of silver nanoparticles on various biological systems. Int J Mol Sci 21(22):8465

Muenraya P, Sawatdee S, Srichana T, Atipairin A (2022) Silver nanoparticles conjugated with colistin enhanced the antimicrobial activity against gram-negative bacteria. Molecules 27(18):5780

Nadhman A, Khan MI, Nazir S, Khan M, Shahnaz G, Raza A, Shams DF, Yasinzai M (2016) Annihilation of Leishmania by daylight responsive ZnO nanoparticles: a temporal relationship of reactive oxygen species-induced lipid and protein oxidation. Int J Nanomed 11:2451

Nie X, Gao F, You W, Chen G, Shao Q, Wang L-H, Huang W-Q, Xia L, Zhang Z, Hong C-Y (2022) Caging pyrophosphate structure blocks the cell wall synthesis to kill bacteria without detectable resistance. Chem Eng J 450:138373

Omar BA, Atif HA, Mogahid ME (2014) Comparison of three DNA extraction methods for polymerase chain reaction (PCR) analysis of bacterial genomic DNA. Afr J Microbiol Res 8(6):598–602

Prabakaran P, Ravindran AD (2011) A comparative study on effective cell disruption methods for lipid extraction from microalgae. Lett Appl Microbiol 53(2):150–154

Quinteros MA, Viviana CA, Onnainty R, Mary VS, Theumer MG, Granero GE, Paraje MG, Páez PL (2018) Biosynthesized silver nanoparticles: Decoding their mechanism of action in Staphylococcus aureus and Escherichia coli. Int J Biochem Cell Biol 104:87–93

Ramzan U, Majeed W, Hussain AA, Qurashi F, Qamar SUR, Naeem M, Uddin J, Khan A, Al-Harrasi A, Razak SIA (2022) New insights for exploring the risks of bioaccumulation, molecular mechanisms, and cellular toxicities of AgNPs in aquatic ecosystem. Water 14(14):2192

Rosli NA, Teow YH, Mahmoudi E (2021) Current approaches for the exploration of antimicrobial activities of nanoparticles. Sci Technol Adv Mater 22(1):885–907

Roy A, Bulut O, Some S, Mandal AK, Yilmaz MD (2019) Green synthesis of silver nanoparticles: biomolecule-nanoparticle organizations targeting antimicrobial activity. RSC Adv 9(5):2673–2702

Saeed S, Tariq P (2009) Antibacterial activity of oregano (*Origanum vulgare Linn*) against gram positive bacteria. Pak J Pharm Sci 22(4):421–425

Shehzad A, Qureshi M, Jabeen S, Ahmad R, Alabdalall AH, Aljafary MA, Al-Suhaimi E (2018) Synthesis, characterization and antibacterial activity of silver nanoparticles using Rhazya stricta. PeerJ 6:e6086

Singh A, Gautam PK, Verma A, Singh V, Shivapriya PM, Shivalkar S, Sahoo AK, Samanta SK (2020) Green synthesis of metallic nanoparticles as effective alternatives to treat antibiotics resistant bacterial infections: A review. Biotechnol Rep 25:e00427

Tang S, Zheng J (2018) Antibacterial activity of silver nanoparticles: structural effects. Adv Healthcare Mater 7(13):1701503

Trombetti F, Minardi P, Mordenti AL, Badiani A, Ventrella V, Albonetti S (2022) The evaluation of the effects of dietary vitamin E or selenium on lipid oxidation in rabbit hamburgers: comparing TBARS and hexanal SPME-GC analyses. Foods. https://doi.org/10.3390/foods11131911

Tsaturyan V, Poghosyan A, Toczyłowski M, Pepoyan A (2022) Evaluation of malondialdehyde levels, oxidative stress and host-bacteria interactions: *Escherichia coli* and salmonella derby. Cells 11(19):2989

Xu H, Qu F, Xu H, Lai W, Andrew Wang Y, Aguilar ZP, Wei H (2012) Role of reactive oxygen species in the antibacterial mechanism of silver nanoparticles on Escherichia coli O157: H7. Biometals 25(1):45–53

Yu Z, Li Q, Wang J, Yu Y, Wang Y, Zhou Q, Li P (2020) Reactive oxygen species-related nanoparticle toxicity in the biomedical field. Nanoscale Res Lett 15(1):1–14

Zhang L, Wu L, Si Y, Shu K (2018) Size-dependent cytotoxicity of silver nanoparticles to Azotobacter vinelandii: Growth inhibition, cell injury, oxidative stress and internalization. PLoS ONE 13(12):e0209020

Zhao Y, Li H, Wei S, Zhou X (2019) Antimicrobial effects of chemical compounds isolated from traditional chinese herbal medicine (TCHM) against drug-resistant bacteria: a review paper. Mini Rev Med Chem 19(2):125–137

Zhou J, Li X-Y, Liu Y-J, Feng J, Wu Y, Shen H-M, Lu G-D (2022) Full-coverage regulations of autophagy by ROS: from induction to maturation. Autophagy 18(6):1240–1255